JOURNAL OF SOLID STATE CHEMISTRY 42, 89–100 (1982)

A Simple Method for the Prediction of New Intermetallic Phases

P. VILLARS AND K. GIRGIS

Institut f. Kristallographie und Petrographie, ETH, CH-8092 Zürich, Switzerland

AND F. HULLIGER

Laboratorium f. Festkörperphysik, ETH, CH-8093 Zürich, Switzerland

Received September 30, 1981

Based on geometrical and electronic regularities we developed a simple interpolation method for the prediction of yet unknown intermetallic phases and tested it on 16 binary and 1 ternary structure types. Starting with hypothetical element combinations the less probable ones are eliminated in various steps, in which the properties of the constituent elements A and B are compared with those of element pairs of the known representatives. For each structure type a linear relation between a short interatomic distance d_{AB} and the concentration-weighted mean atomic radius $\bar{R}$ is used to establish a relation between the lattice constants and the radii R_A and R_B of the involved atoms. A generalized space-filling factor can then be formulated as a function of $\bar{R}$ and R_A/R_B. A first coarse selection is based on space filling in the R_A/R_B vs $\bar{R}$ diagram. The final reduction of the potential candidates is carried out in diagrams which involve the electronic properties of the elements.

1. Introduction

Modern industry is highly interested in new materials which possess optimal properties. Certain structure types appear to be favored for special applications, such as the A15 structure for superconductivity. People engaged in materials research therefore are interested in guide lines for the synthesis of new representatives of particular structure types. For the synthesis of metallic alloy phases about 80 elements have to be considered: If we exclude the halogens, the inert gases, and the actinides beyond number 93 (Np), we are left with 84 elements, which for each binary structure type A_mB_n offer the formal possibility of 6972 combinations. For choosing the most reasonable candidates one usually has to rely on a mixture of feeling and trial and error.

Recently Savitskii and co-workers (*1–5*) introduced a sophisticated prognosis method for the prediction of new members of various alloy structure types. For this purpose the properties of the elements, as well as of the known representatives of a structure type, are represented in a multidimensional diagram. An appropriate computer program was developed which recognizes a pattern in this space, dividing the element combinations into three categories: Combinations inside the pattern are likely to exist in this structure, while those outside will probably adopt another structure, and those on the border line are indiscernible.

0022-4596/82/040089-12$02.00/0

Based on this procedure the following numbers of probable element combinations have been predicted: $MgCu_2$ type Laves phases 2000 (*4*), $CaCu_5$ type 1100 (*4*), $SiCr_3$ (β-W) type 714 (*3*), CsCl type 1500 (*5*), and σ-phase type 156 (*2*). Although characteristic data of the elements were used, the resulting numbers of new representatives are surprisingly high. Thus, one gets the impression that the extrapolation might have been driven too far.

On searching for regularities among the representatives of 17 structure types that occur with Nb, Ta–Group IIIb and IVb binary compounds, we found that the number of possible new combinations can be reduced to about one-quarter of those given by Savitskii and co-workers by considering empirical geometric and electronic characteristics.

2. Regularities Exhibited by Alloy Structure Types

The derivation of empirical structural relations, which are not based only on a hard-sphere model, requires the knowledge of a certain number of existing representatives. A great part of the physical and chemical requirements for the occurrence of a certain structure is contained in the structural characteristics such as axial ratios and space filling, provided that these parameters do not show a broad scatter. If the available experimental data permit us to derive with sufficient accuracy a relation between the structural characteristics and the size of the engaged atoms, we are able to calculate the hypothetical unit cell of any new compound.

Of course, the value of these speculations increases (and the number of possible new phases decreases) with the more electronic information we consider. Moreover, predictions based on interpolation are fairly trustworthy, while those gained by extrapolation become more and more speculative the farther away we move from the basal points. In fact, it is rather arbitrary where we draw our border lines. We admit that interpolations are more of a practical value whereas the speculative extrapolations are more interesting theoretically. Our interpolation method thus will not lead to new subgroups of a structure type.

From the 17 structure types listed in Table 1 the following regularities have been deduced. These regularities will be used to develop our prognosis method. In advance we discuss these regularities in detail.

(1) A linear d_{AB} vs $\bar{R}$ dependence and a linear V_{uc} vs $\bar{V}$ dependence exists for these alloy structures. Here, d_{AB} designates a shortest distance[1] between atom A and atom B that depends on all lattice constants. V_{uc} is the unit-cell volume and $\bar{R}$ and $\bar{V}$ are concentration-weighted mean atomic radii and volumes respectively,

$$\bar{R} = (mR_A + nR_B)/(m + n),$$
$$\bar{V} = (mV_A + nV_B)/(m + n),$$

for the compounds A_mB_n, where we always take $m < n$. We used $\bar{R}$ rather than $(R_A + R_B)/2$ because we found experimentally a much better linearity of the d_{AB} dependence. For R_A and R_B we used the metallic radii proposed by Teatum *et al.* (*6*), listed also in Pearson's book (*7*).

(2) There is a narrow range for the values of axial ratios c/a and b/a and the generalized space-filling factor for all representatives of these structure types. This property is in fact essential for our purpose. In certain cases of pronounced scatter of the axial

[1] In a three-dimensional structure one might as well choose any other A–B distance (with a likewise good linear regression factor) since the structure is a steric framework that reflects the stoichiometry as well as the kind of participating atoms. If in the structure the atomic positions of A and B contain free parameters, then reliable sets x_A, y_A, z_A and x_B, y_B, z_B are chosen equal for all representatives, as in most cases these parameters were not determined.

TABLE I

SUMMARY OF THE PROCEDURE AND RESULTS OF OUR PROGNOSIS METHOD APPLIED TO 17 STRUCTURE TYPES

Structure type A_mB_n	Space group	Atomic positions used for d_{AB}: A x	A y	A z	B x	B y	B z	d_{AB} (Å)	Linear regress. factor	$\overline{c/a}$ $\overline{(b/a)}$	Space-filling range	$\bar{R}$ range (Å)	R_A/R_B range	Element combinations A–B*	N_o	$N_{pr.}$
σ-CrFe	$P4_2/mnm$	0.318	0.318	0.25	0.065	0.262	0	1.991 $\bar{R}$ + 0.005	0.992	0.52 ± 0.01	0.735–0.75	1.2 –1.6	0.8 –1.2	d^{1-5}–d^{5-10} [a]	48	50
α-Mn	$I\bar{4}3m$	0.317	0.317	0.317	0.356	0.356	0.042	1.990 $\bar{R}$ − 0.090	0.996	1.0	0.74 –0.765	1.25–1.7	0.7 –1.3	p,d–d; f–s [b]	31	10
Ga_4Ti_5	$P6_3/mcm$	0.620	1	0.25	0.333	0.667	0	2.297 $\bar{R}$ − 0.489	0.985	0.69 ± 0.01	0.72–0.785	1.35–1.7	0.7 –1.05	p–d	6	22
Si_2U_3	$P4/mbm$	0.389	0.889	0	0.181	0.681	0.5	1.944 $\bar{R}$ − 0.069	0.989	0.52 ± 0.01	0.715–0.82	1.15–1.7	0.6 –1.0	s–d; p–d, f	18	67
Si_3W_5	$I4/mcm$	0	0	0.25	0.074	0.223	0	1.909 $\bar{R}$ − 0.033	0.992	0.50 ± 0.01	0.745–0.78	1.25–1.95	0.75–1.10	p–d, f*	44	156
B_3Cr_5	$I4/mcm$	0.375	0.875	0	0.166	0.666	0.150	1.692 $\bar{R}$ + 0.228	0.998	1.86 ± 0.03	0.725–0.86	1.7 –2.1 1.10–1.8	0.6 –0.9 0.7 –1.10	$p,d^{9,10}$–s; [d] p–d, f	37	183
Si_3Mn_5	$P6_3/mcm$	0.25	0	0.25	0.401	0	0.75	2.496 $\bar{R}$ − 0.688	0.982	0.70 ± 0.02	0.645–0.825	1.25–1.85†	0.65–1.2†	p–s, d, f; d^{6-8}–f; d^{5-10}–d^{1-5}	162	481
$ZrSi_2$	$Cmcm$	0	0.102	0.25	0.5	0.053	0.75	1.965 $\bar{R}$ − 0.065	0.885	0.99 ± 0.02 (3.91 ± 0.09)	0.705–0.75	1.3 –1.8	0.95–1.4	d, f–p	19	59
$CuMg_2$	$Fddd$	0	0	0.128	0.081	0.25	0.25	1.952 $\bar{R}$ − 0.224	0.999	1.97 ± 0.03 (0.58 ± 0.02)	0.74 –0.79	1.2 –1.7	0.6 –1.0	d–p, s	6	27
$CuAl_2$	$I4/mcm$	0.5	0.5	0.25	0.160	0.660	0	1.840 $\bar{R}$ + 0.052	0.987	0.82 ± 0.03	0.725–0.80	1.1 –1.85	0.6 –1.0	p–d, f; d–p, d; d^{7-10}–f[e]	47	384
$CrSi_2$	$P6_122$	0.5	0	0.5	0.680	0.159	0.166	1.543 $\bar{R}$ + 0.224	0.995	1.39 ± 0.02	0.765–0.815	1.25–1.65	0.9 –1.2	d–p	10	22
$TiAl_3$	$I4/mmm$	0	0	0	0	0.5	0.25	2.242 $\bar{R}$ − 0.337	0.978	2.15 ± 0.11	0.755–0.81	1.2 –1.55	0.85–1.25	d^{1-5}–d, p	16	50
PFe_3	$I\bar{4}$	0.286	0.048	0.480	0.168	0.220	0.752	1.711 $\bar{R}$ + 0.070	0.994	0.50 ± 0.003	0.74 –0.765	1.15–1.65	0.8 –1.1	p–d	12	58
$SnNi_3$	$P6_3/mmc$	0.333	0.667	0.25	0.167	0.333	0.75	1.684 $\bar{R}$ + 0.394	0.983	0.79 ± 0.04	0.72 –0.85	1.2 –1.85	0.9 –1.4	d–s; d^1, f–p d^{1-5}–d^{5-10} [f]	56	206
$AuCu_3$	$Pm3m$	0	0	0	0	0.5	0.5	1.817 $\bar{R}$ + 0.232	0.971	1.0	0.735–0.865	1.2 –1.85	0.7 –1.45	p–s, f; s, d, f–p s, p, d, f–d [g]	190	510
$SiCr_3$	$Pm3n$	0	0	0	0.25	0	0.5	1.783 $\bar{R}$ + 0.276	0.989	1.0	0.725–0.795	1.25–1.7	0.78–1.3	p,d–d^{1-5} [h]	91	138
$AlCr_2C$	$P6_3/mmc$	0.333	0.667	0.75	0.667	0.333	0.914	1.774 $\bar{R}$ − 0.031	0.935	4.38 ± 0.12	0.72 –0.80	1.3 –1.7	0.75–1.2	p,d^{10}–d	36	82

Note. N_o = Number of known representatives on which the prognosis is based, $N_{pr.}$ = number of predicted representatives.

* s, p, d^n, f are used to designate the groups of the periodic system: s = alkali and alkaline-earth elements, p = elements of Group IIIB to VIB (boron to oxygen group), d = transition elements, starting with the Sc group (d^1) and including the Cu (d^9) and Zn group (d^{10}), f = rare earth elements, including Y and the actinides. Exceptions: (*a*) VTa, $AlNb_2$, $AlTa_2$; (*b*) $Al_{12}Mg_{17}$; (*c*) Pt_5Ca_5, Au_3Cd_5; (*d*) Ag_3Yb_5; (*e*) $AuNa_2$; (*f*) ($AlCe_3$); (*g*) $IrHf_3$, $MnZr_3$; (*h*) Cr_3O, Mo_3O, W_3O, Mo_3Be.

† For p–s combinations $\bar{R}$ = 1.7–2.1 and R_A/R_B = 0.6–0.9.

ratios the structure family may be subdivided, as, e.g., for CaC_2–$MoSi_2$–$AlCr_2$–$PdBi_2$ (*h*) and loellingite ($FeAs_2$)–marcasite (FeS_2). These varieties are the result of a different bonding character. Special cases are the NiAs– and CdI_2-type phases.

One of the consequences from the two above-mentioned regularities is the existence of a narrow grouping formed by the representatives of a certain structure type in a generalized iso-space-filling $\bar{R}$–R_A/R_B diagram. A deduction of this diagram is presented below.

The structural information derived from the known compounds (*14*) and used for the hypothetical compounds is derived as follows.

The short interatomic distance

$$d_{AB} = a[(x_A - x_B)^2 + (y_A - y_B)^2(b/a)^2 + (z_A - z_B)^2(c/a)^2 + 2(y_A - y_B)(z_A - z_B)(bc/d^2)\cos\alpha + 2(x_A - x_B)(z_A - z_B)(c/a)\cos\beta + 2(x_A - x_B)(y_A - y_B)(b/a)\cos\gamma]^{1/2}$$

is determined for all the known representatives (using the same set of reliable site-parameter values x°, y°, z°) and plotted as a function of $\bar{R}$. A linear dependence

$$d_{AB} = k_1\bar{R} + k_2$$

will result. The constant $k_2 \neq 0$ is reflecting the compressibility of the atoms, and this makes the difference to a hard-sphere model. The lattice constants of any hypothetical compound now can be calculated as

$$a \approx (k_1\bar{R} + k_2)[(x_A^\circ - x_B^\circ)^2 + (y_A^\circ - y_B^\circ)^2(\overline{b/a})^2 + (z_A^\circ - z_B^\circ)^2(\overline{c/a})^2 + 2(y_A^\circ - y_B^\circ)(z_A^\circ - z_B^\circ)(\overline{bc/a^2})\cos\alpha + 2(x_A^\circ - x_B^\circ)(z_A^\circ - z_B^\circ)(\overline{c/a})\cos\beta + 2(x_A^\circ - x_B^\circ)(y_A^\circ - y_B^\circ)(\overline{b/a})\cos\gamma]^{-1/2} = (k_1\bar{R} + k_2)/\Delta,$$

$$b \approx a(\overline{b/a}) = (k_1\bar{R} + k_2)(\overline{b/a})/\Delta,$$

$$c \approx a(\overline{c/a}) = (k_1\bar{R} + k_2)(\overline{c/a})/\Delta.$$

As an example we treat the monoclinic system. The space filling $SF = Z(mV_A + nV_B)/V_{uc}$ can be generalized as

$$SF = \frac{(4\pi/3)\, Z\, \Delta^3\, (mR_A^3 + nR_B^3)}{(k_1\bar{R} + k_2)^3(\overline{b/a})(\overline{c/a})\sin\bar{\beta}}.$$

The above formula can be rewritten as

$$\bar{R}_{(R_A/R_B)}\Big|_{\text{const } SF} = \frac{k_2[SF\,(\overline{b/a})(\overline{c/a})\sin\bar{\beta}]^{1/3}[m + n\,(R_A/R_B)^{-1}]}{(m+n)\,\Delta\,\{(4\pi/3)\,Z\,[m + n(R_A/R_B)^{-3}]\}^{1/3} - k_1\{[SF(\overline{b/a})(\overline{c/a})\sin\bar{\beta}]^{1/3}\,[m + n(R_A/R_B)^{-1}]\}},$$

whereby k_1,k_2 = constants from the linear regression $d_{AB} = k_1\bar{R} + k_2$, Z = number of formula units, m,n = stoichiometric proportions, $\overline{c/a}$, $\overline{b/a}$, $\bar{\beta}$ = mean values of the representatives for a certain structure type, and $\Delta = [(x_A^\circ - x_B^\circ)^2 + (y_A^\circ - y_B^\circ)^2(\overline{b/a})^2 + (z_A^\circ - z_B^\circ)^2(\overline{c/a})^2 + 2\,(x_A^\circ - x_B^\circ)(z_A^\circ - z_B^\circ)(\overline{c/a})\cos\bar{\beta}]^{1/2}$.

With this expression we calculate the iso-space-filling net in the R_A/R_B vs $\bar{R}$ diagram.

(3) The electronic characteristics of a structure type are reflected in a grouping in a plot of $\overline{VE}$ vs Δx, where $\overline{VE} = (mVE_A + nVE_B)/(m + n)$ is the mean valence-electron concentration and $\Delta x = x_A - x_B$ is the electronegativity difference. We used the x values given by Thomas and Gordy (*8*).

(4i) There is a unique (in some cases trivial) relation between the position of the elements in the periodic table and their equipoint occupation in the structure.

(4ii) There is a narrow grouping for the representatives of a given structure type in an isostoichiometric diagram of binary ele-

ment combinations. In such a diagram we arrange the elements according to their number of s, p, d, and f electrons, the A elements along the vertical axis and the B elements along the horizontal axis. In a diagram we plot VE_A vs VE_B, where VE_A and VE_B are the numbers of valence electrons of element A and element B, respectively. Only the chemical valence electrons are counted in the case of the rare earth elements. Ce, (Sm), Eu, Yb, and U may be problematic in some cases.

The results of our analysis of 17 structure types are summarized in Table 1.

3. The Principle of Our Prognosis Method

Based on these four regularities we are now going to describe our prediction method in detail on the examples of the σ structure type (σ phase) and of the $SiCr_3$ structure type. Polyhedron packings of these structure types are shown in Figs. 1 and 6 (*9, 10*).

We approximate the compositions of the σ phases A_xB_y with a 1 : 1 stoichiometry, although pronounced deviations are possible. This is a weak point, but consideration of variable stoichiometry would make the treatment too tedious.

The σ-phase structure is described in space group $P4_2/mnm$ and the equivalent positions are

A: 2(a) 0, 0, 0; $\frac{1}{2}$, $\frac{1}{2}$, $\frac{1}{2}$,
B: 4(g) ± (x, $\bar{x}$, 0; $\frac{1}{2}+x$, $\frac{1}{2}+x$, $\frac{1}{2}$),
C: 8(i) ± (x, y, 0; y, x, 0; $\frac{1}{2}+x$, $\frac{1}{2}-y$, $\frac{1}{2}$; $\frac{1}{2}+y$, $\frac{1}{2}-x$, $\frac{1}{2}$),
D: 8(i) as above, and
E: 8(j) ± (x, x, z; x, x, $\bar{z}$; $\frac{1}{2}+x$, $\frac{1}{2}-x$, $\frac{1}{2}+z$; $\frac{1}{2}+x$, $\frac{1}{2}-x$, $\frac{1}{2}-z$).

A elements are in position **B**: 4(g), while B elements only are found in positions **A**: 2(a) and **D**: 8(i). The positions **C** and **E** can be occupied by both the A elements and the B elements (*17*).

The shortest distance between the A

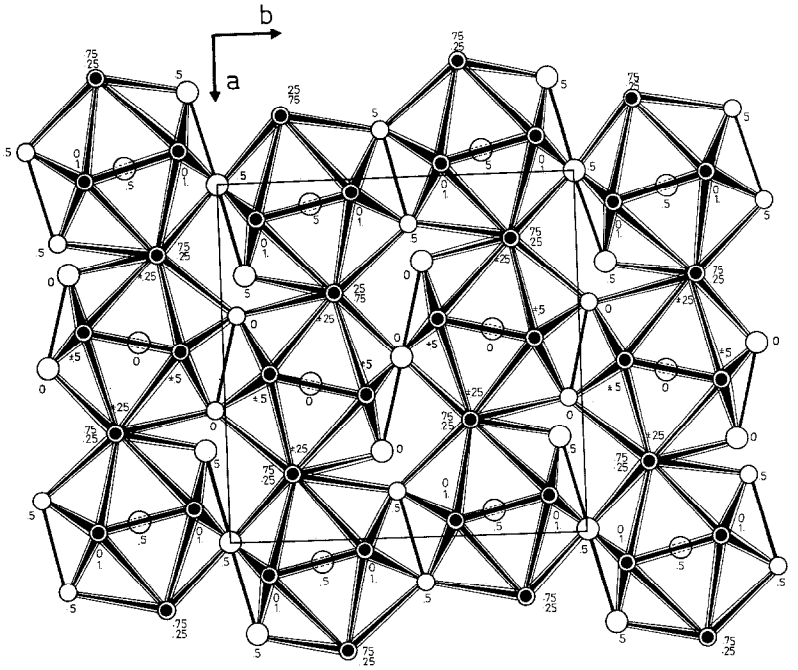

FIG. 1. Polyhedron packing of the σ-CrFe structure type (*10*).

atom (Cr in **E**: 8(j) at 0.318, 0.318, 0.25) and the B atom (Fe in **C**: 8(i) at 0.065, 0.262, 0) is

$$= a[0.0665 + 0.0625\ (c/a)^2]^{1/2}.$$

A plot of the experimental data for d_{AB} vs $\bar{R}$ for all the known σ phases (Fig. 2) leads to

$$d_{AB}\ (\text{Å}) = 1.991\ \bar{R} + 0.005.$$

This linear dependence is obeyed with a rather high regression factor of 0.992. A linear dependence also exists between V_{uc} and $\bar{V}$, but we do not use it further.

For the σ-CrFe-type unit cells the mean value of the axial ratio is $\overline{c/a} = 0.52 \pm 0.01$ (0.01 being the statistical deviation). The generalized space filling SF is

$$SF_{\sigma\text{-CrFe}} = \frac{(4\pi/3)\ 15\ [0.0665 + 0.0625\ (\overline{c/a})^2]^{3/2}(R_A^3 + R_B^3)}{(1.991\ \bar{R} + 0.005)^3(\overline{c/a})}.$$

This formula is generalized and rewritten in order to construct the parameter net SF = const in Fig. 3:

$$\bar{R}_{(R_A/R_B)}\Big|_{\text{const } SF} = \frac{0.005[SF\ 0.52]^{1/3}[1 + (R_A/R_B)^{-1}]}{2\ [0.0665 + 0.0625(0.52)^2]^{1/2}\{(4\pi/3) \cdot 15\ [1 + (R_A/R_B)^{-3}]\}^{1/3} - 1.991\{[SF\ 0.52]^{1/3}[1 + (R_A/R_B)^{-1}]\}}.$$

Iso-space-filling is used as a parameter in Fig. 3, which shows an R_A/R_B vs $\bar{R}$ plot with the known and the predicted σ phases. The experimental values for the space-filling factor SF scatter within the range 0.735–0.75. Thus, iso-space-filling $SF \leq 0.75$ and a mean radius $1.2 \leq R \leq 1.6$ Å were assumed as a reasonable border line. The SF limit coincides with an R_A/R_B range of 0.8–1.2. The broken curve defines a smaller field which contains all the predicted phases that escaped the final purgation step.

The second reduction takes place in the $\overline{VE}$ vs Δx diagram. Besides the known compounds, we have indicated in Fig. 4 all the hypothetical compounds that fulfill our geometrical criteria. Surprisingly, the crosses

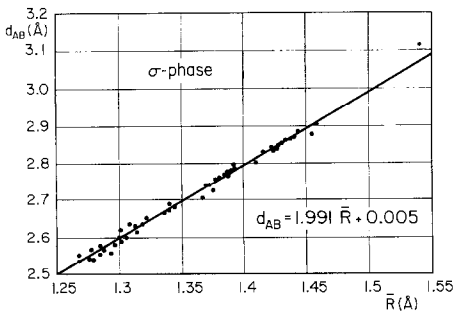

FIG. 2. The linear dependence between the shortest distance d_{AB} and the mean radius $\bar{R}$ for the σ phases. The position of atom A is x, x, z, with $x_A = 0.318$ and $z_A = 0.25$, and that of atom B is $x, y, 0$, with $x_B = 0.065$ and $y_B = 0.262$.

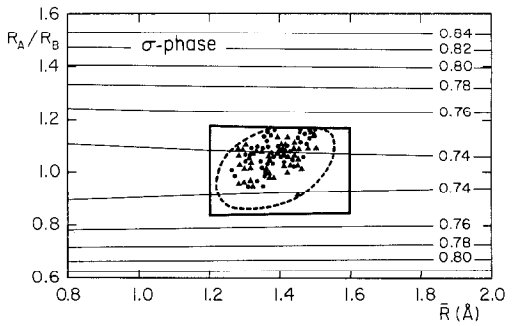

FIG. 3. The geometric field of existence of the σ-CrFe-type phases. The parameter net represents the generalized space-filling factor SF. Triangles stand for existing phases, dots for predicted phases that survived all purgation processes. The preliminary area of existence, based on space filling and mean radius (full curves), can therefore be reduced to that within the dotted curve.

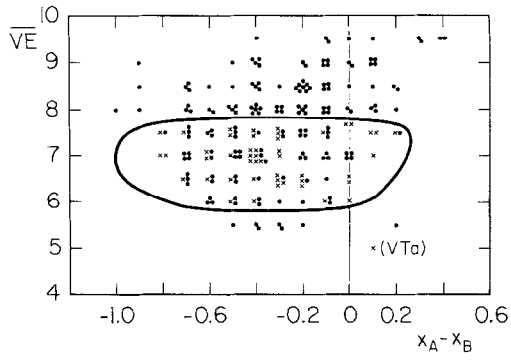

FIG. 4. The electronic diagram $\overline{VE}$ vs Δx for the σ phases. Existing compounds are indicated by crosses, geometrically permitted compounds by dots. All candidates outside the curve are discarded.

designating the known σ phases are crowded all together, with one exception, VTa. The most probable hypothetical σ phases are those lying within the curve. Even by cutting off only the phases with $\overline{VE} \geq 8$ we reduce the number of predicted phases by more than a factor of two.

The components of the known σ phases A_xB_y belong to the following group:

d^{1-5} elements (A) combined with d^{5-10} elements (B).

Figure 5 is a graphical representation of point (4ii). It was used for a final reduction

TABLE II

PROGNOSIS TABLE FOR σ PHASES

B elements

A elements	Mn	Tc	Re	Fe	Ru	Os	Co	Rh	Ir	Ni	Pd	Pt	Cu	Ag	Au	Zn	Cd	Hg
Ti	⊕			C	C	+	C	+	C	C	+	C						
Zr			⊕			+			⊕		C	C						
Hf					+	+		+	C		+	+						
V	⊕	+	⊕	⊕	C	+	⊕	+	C	⊕	C	+						
Nb	+	+	⊕	⊕	+	⊕	C	⊕	⊕	C	⊕	⊕						
Ta	+	+	⊕	C	C	⊕	+	⊕	⊕	C	⊕	⊕			⊕			
Cr	⊕	⊕	⊕	⊕	⊕	⊕	⊕	+	+	⊕								
Mo	⊕	⊕	⊕	⊕	⊕	⊕	⊕	+	⊕									
W	T	⊕	⊕	C	⊕	⊕	⊕	C	⊕									
Mn	+	⊕	⊕	C	E	+												
Tc		+	T	⊕	S	T												
Re			+	⊕	T	T												

Note. Symbols: ⊕, known representatives on which we based our prognosis; ■, compounds predicted by Savitskii and Gribulya (*2*); +, compounds predicted in this work [if further information is available from phase diagrams, C, I, S, T, or E is given instead of + (*11–13, 16*)]; C, compounds occurring with other compositions only, according to phase diagram; I, complete insolubility according to phase diagram; S, complete solubility according to phase diagram; E, eutectic/peritectic system without any compounds formed; T, thermodynamically unstable according to Miedema (*18*).

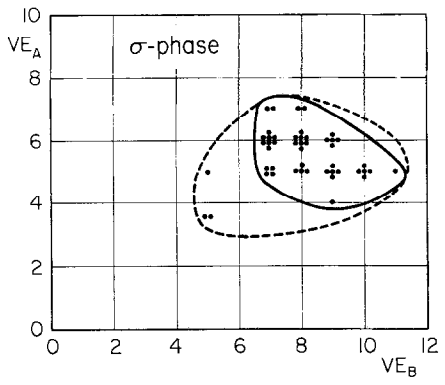

FIG. 5. The field of existence of the σ phases in a valence-electron concentration diagram. The known representatives are given by dots. The three exceptions with $VE_B = 5$ induce a much larger allowed area.

of the number of candidates. Those which fall within the heavy black curve appear to be almost safe.

Thus, starting with 48 σ-CrFe-type representatives the geometrical interpolation leads to 198 possible new combinations. This number is further reduced in a $\overline{VE}$ vs Δx diagram to 62, and finally in a VE_A vs VE_B diagram 50 candidates survive. These are listed in Table 2. On the basis of thermodynamical considerations, Miedema (*18*) predicted stable element combinations and ruled out unstable combinations. Some of these unstable phases may exist under high pressure. If we eliminate them we are left with 46 potential σ-phase candidates.

Various detailed studies have been published on the $SiCr_3$ (A15, β-W)-type compounds (*19–26*) and "it is believed that all reasonably stable A15 phases have been found" (*25*). Nevertheless, we demonstrate our method on this structure type for comparison.

The $SiCr_3$ structure type is described in space group $Pm3n$ and the equivalent positions are

Si in 2(*a*): 0, 0, 0; $\frac{1}{2}$, $\frac{1}{2}$, $\frac{1}{2}$,
Cr in 6(*c*): $\pm$ ($\frac{1}{4}$, 0, $\frac{1}{2}$; $\frac{1}{2}$, $\frac{1}{4}$, 0; 0, $\frac{1}{2}$, $\frac{1}{4}$).

The shortest distance between the *A* atom at (0, 0, 0) and the *B* atom at ($\frac{1}{4}$, 0, $\frac{1}{2}$) is

$$d_{AB} = 0.5590\ a.$$

This expression holds exactly, as the structure contains no free parameters. A plot of the experimental data for the known $SiCr_3$-type phases leads to the relationship

$$d_{AB}\ (\text{Å}) = 1.783\ \bar{R} + 0.276.$$

This linear dependence is obeyed with a high regression factor of 0.989 (see Fig. 7). The space-filling factor thus can be written

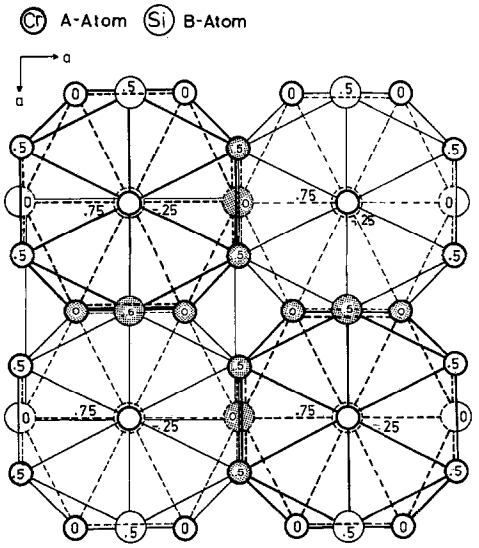

FIG. 6. Polyhedron packing of the $SiCr_3$ structure.

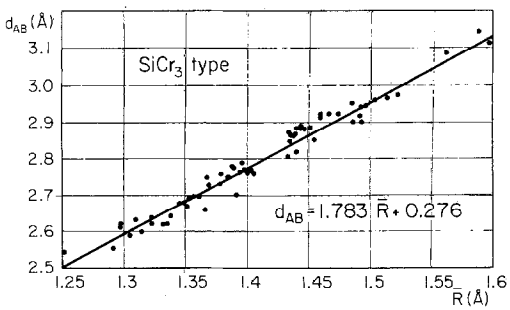

FIG. 7. The linear dependence d_{AB} vs $\bar{R}$ for the $SiCr_3$-type phases. Atom *A* at (0, 0, 0), atom *B* at ($\frac{1}{4}$, 0, $\frac{1}{2}$), hence $d_{AB} = 0.5590\ a$.

as

$$SF_{SiCr_3} = \frac{(4\pi/3)\ 2\ (0.559)^3(R_A^3 + R_B^3)}{(1.783\ \bar{R} + 0.276)^3}\ .$$

This formula is generalized and rewritten in order to construct the parameter net SF = const in Fig. 8:

$$\bar{R}_{(R_A/R_B)}\Big|_{\text{const } SF} = \frac{0.276\ [SF]^{1/3}[1 + 3\ (R_A/R_B)^{-1}]}{2.236\ \{(4\pi/3) \cdot 2[1 + 3\ (R_A/R_B)^{-3}\}^{1/3} - 1.783\{[SF]^{1/3}[1 + 3(R_A/R_B)^{-1}]\}}\ .$$

The experimental points all lie within a space-filling range of 0.725–0.795. As additional limits we choose R_A/R_B = 0.78 and 1.3.

The component elements of the known $A15$ phases AB_3 belong to the following two groups:

p elements (A) with d^{1-5} elements (B),

d elements (A) with d^{1-5} elements (B).

The ratio of the p and d elements to the d^{1-5} elements is fairly close to 1 : 3.

The electronic characteristics of the $A15$ phases are quite pronounced. In the $\overline{VE}$ vs Δx diagram (Fig. 9) the existing representatives are given by crosses, those predicted from the R_A/R_B vs $\bar{R}$ diagram by dots. More than half the dots lie outside the area defined by the known representatives.

In the VE_A vs VE_B diagram (Fig. 10) the existence field for the $A15$ compounds might well be singly connected as indicated by the broken contours. If we restrict our interpolation area to the two fields within the heavy curves we loose another 65 candidates.

Thus starting from 91 known representatives the geometrical criteria lead to 520 new candidates. Of these, 244 survive the sieving process in the $\overline{VE}$ vs Δx diagram, and only 133 candidates are left in the VE_A vs VE_B diagram. Finally, Miedema's thermodynamic stability criteria eliminate 45 combinations, so that we end up with 93 fairly trustworthy new candidates listed in Table 3.

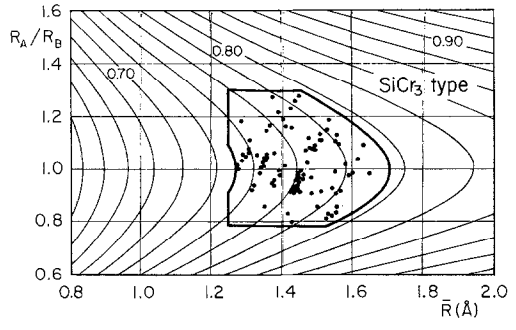

FIG. 8. Field of existence of the $SiCr_3$-type phases in the R_A/R_B vs $\bar{R}$ diagram. The existing compounds (dots) lie within the space-filling values 0.75 and 0.795 and adopt R_A/R_B values between 0.78 and 1.3.

4. Limits of Our Prognosis Method

In order to obtain reliable prognosis results, the following conditions should be fulfilled:

1. A minimum of about 10 representa-

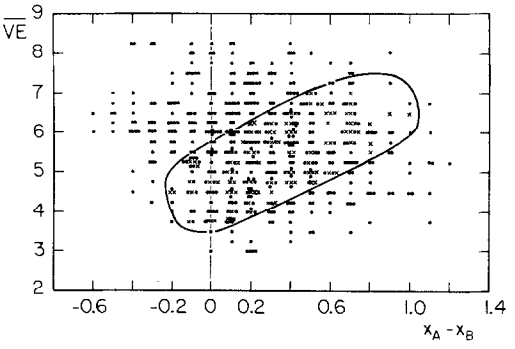

FIG. 9. Mean valence-electron concentration vs electronegativity difference for the known (crosses) and the geometrically permitted (dots) $SiCr_3$-type phases. The field of existence is reduced by the closed curve.

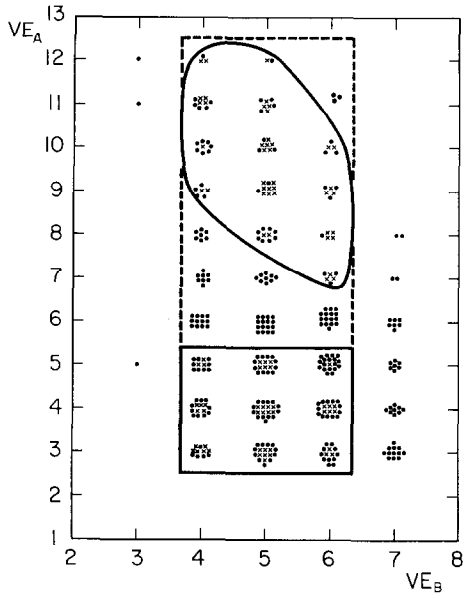

FIG. 10. Valence-electron numbers VE_A, VE_B of the atoms A and B in $SiCr_3$-type phases AB_3. Existing phases: crosses; predicted compounds as deduced from Fig. 9: dots. The less speculative field of existence is framed by heavy lines.

tives of the considered structure type should be known.

2. The linear regression factor of the d_{AB} vs $\bar{R}$ dependence should be higher than 0.98.

3. The c/a and b/a ratios should not vary more than $\pm 5\%$ of the mean value. Similar conditions should hold for the angles α, β, and γ.

4. The space-filling range should not be larger than 0.1.

5. The representatives of a structure type should form a closed group in the $\overline{VE}$ vs Δx diagram, as well as in the VE_A vs VE_B diagram.

6. Among the compounds with rare earth and actinide elements, those with Ce, Sm, Eu, Yb, U, etc., may require a special treatment since these elements can occur with different valences.

As can be seen in Table 1 some structure types contain exceptions, i.e., existing members which fall distinctly beyond the border lines either in the geometrical diagram or in the electronic diagrams. These exceptions may be due to inaccuracies of the parameters used, or else they may point to new subgroups. Thus, in the case of the Si_3W_5-type family, the group of the p and f element combinations has been discovered only recently, while only the group of the p and d element combinations was known before.

5. Discussion

The prognosis originally was based on the data compiled by Pearson (1967, *14*). Of 97 new compounds reported in the following 12 years 96 have been predicted correctly by our method.

It is interesting to compare the results of our simple prognosis method with the sophisticated computer method of Savitskii and co-workers (*1–5*). While Savitskii and Gribulya (*2, 3*) predicted 714 new $SiCr_3$-type compounds and 156 new σ phases, our corresponding figures are 93 and 46, respectively. Seventy-nine percent of our candidates are identical with Savitskii and Gribulya's (see Tables 2 and 3).

Our method is described here for binary compounds. It can be applied as well to ternary phases provided that only two elements are varied, e.g., in ternary carbides, etc. As an example we have listed in Table 1 our results for the $AlCr_2C$-type phases.

In general we can reduce the number of predicted phases with our prognosis to twice or three times the known intermetallic compounds of a treated structure type. The predicted phases should be understood as a "first selection" of the hypothetical possible combinations. There are different regularities which are only valid for a limited number of structure types. These can be applied to our predicted phases. In this way one can reduce these to the most probable expected compounds, as shown in the following examples.

Savitskii and Gribulya (*3*) found the rule

TABLE III

PROGNOSIS TABLE FOR THE $SiCr_3$-TYPE PHASES

A elements

B elements	B	Al	Ga	In	Tl	C	Si	Ge	Sn	Pb	N	P	As	Sb	Bi	O	S	Se	Te	Po	Sc	Y	Ti	Zr
Ti			*⊕	S	⊕		6	+	⊕	S				⊕	+								+	T
Zr		*⊕	⊕	S	⊕		⊕	⊕	⊕	⊕				*⊕	⊕		+						T	+
Hf		C	C	+	+					+											T		T	S
V		⊕	⊕	⊕	⊕		⊕	⊕	⊕	⊕			⊕	⊕	⊕								S	+
Nb		⊕	⊕	⊕	⊕		⊕	⊕	⊕	⊕		2	6	⊕	⊕				⊕		T		T	T
Ta		C	⊕	T	T		⊕	⊕	⊕	T		2		⊕	E						T		T	T
Cr		C	⊕	T			⊕	⊕	E			1	⊕	C	E	⊕					T		C	C
Mo		⊕	⊕	T	T		⊕	⊕	⊕	T		1	+		T	⊕	+				T		S	C
W		ø	T	T	T		⊕	C	T	T		1		T	T	⊕					T		E	C

	Hf	V	Nb	Ta	Cr	Mo	W	Mn	Tc	Re	Fe	Ru	Os	Co	Rh	Ir	Ni	Pd	Pt	Cu	Ag	Au	Zn	Cd	Hg
Ti	T		T	T										C		⊕	C	C	⊕		⊕	⊕			⊕
Zr	S	+		T										3	C	7/⊕	C		C	4	*⊕	⊕			⊕
Hf	+		T	T												6		C	C	C	C	C			+
V	C	+	S								C		⊕	⊕	Ø	⊕	⊕	⊕	⊕	T	T	⊕		⊕	T
Nb	T	S	+	T									⊕		⊕	⊕		C	⊕			⊕			
Ta	T	C	T	+							C		7	C	7	7/⊕	C	7	⊕	+	T	⊕			T
Cr	C		C	C	+				+	C		⊕	⊕		⊕	⊕		ø	⊕						
Mo	C	T	T	S					⊕	⊕			⊕		C	⊕			⊕						
W	C	S	S	S			+		C	⊕			⊕		C	C			N		T				

Note. Symbols: ⊕, known representatives on which we based our prognosis; ■, compounds predicted by Savitskii and Gribulya (*3*); +, compounds predicted in this work [if further information is available from phase diagrams, C, I, S, E, T, *, or a number is given instead of + (*11–13, 16*)]; C, only compounds with other stoichiometric proportions known according to phase diagram; I, complete insolubility according to phase diagram; S, complete solubility according to phase diagram; E, eutectic/peritectic system without any compound formed; *, AB_3 phase of unknown structure reported; Ø, structure type with less than three representatives; 1, PFe_3 type; 2, PTi_3 type; 3, BRe_3 type; 4, $CuTi_3$ type; 5, $SnNi_3$ type; 6, $AuCu_3$ type; 7, σ phase; T, thermodynamically unstable according to Miedema (*18*).

"In systems with a σ-phase there also exist phases of the $SiCr_3$, Laves ($MgZn_2$), and CsCl type which may be called concomitants of the forecast structure."

The Darken–Gurry diagram and the "electronegative" and "relative valence effect" rules of Hume–Rothery treated in the paper of Waber *et al.* (*27*) are helpful for deciding whether we have to expect complete solubility of two elements or not.

Even the information given in Tables 2 and 3, which are taken from the known binary phase diagrams (*11–13, 16*), are helpful for deciding which of the predicted phases are the most probable ones.

We may stress that our predicted phases need not exist, but these are the most probable ones because they have geometric and electronic characteristics similar to those of the known representatives of the consid-

ered structure type.

Of course our prognosis method as presented here can be developed further if one finds a new grouping in another diagram. Such a new grouping of the representatives of the $SiCr_3$, CFe_3, PTi_3, and PFe_3 types was, for example, found in a melting-point sum of the element A and B ($T_A + T_B$) vs T_A/T_B diagram.

References

1. E. M. SAVITSKII AND V. B. GRIBULYA, *J. Phys. Chem. Solids* **33,** 1853 (1972).
2. E. M. SAVITSKII AND V. B. GRIBULYA, *Dokl. Akad. Nauk SSSR* **220,** 1066 (1975). [English transl. *Doklady Technical Physics* **220,** 129 (1975)]
3. E. M. SAVITSKII AND V. B. GRIBULYA, *Dokl. Akad. Nauk SSSR* **223,** 1383 (1975). [English transl. *Doklady Chemistry* **223,** 414 (1975)]
4. E. M. SAVITSKII, V. B. GRIBULYA, AND N. N. KISELYOVA, *J. Less-Common Met.* **72,** 307 (1980).
5. E. M. SAVITSKII, in "Intermetallische Phasen" (Autorenkollektiv, Ed.), Deut. Verlag Grundstoffindustrie, Leipzig (1976).
6. E. TEATUM, K. A. GSCHNEIDNER, AND J. T. WABER, LA-2345, U.S. Dept. of Commerce, Washington, D.C. (1960).
7. W. B. PEARSON, "The Crystal Chemistry and Physics of Metals and Alloys," p. 151, Wiley–Interscience, New York (1972).
8. W. GORDY AND W. J. O. THOMAS, *J. Chem. Phys.* **24,** 439 (1956).
9. K. K. BHANDARY AND K. GIRGIS, *Acta Crystallogr. Sect. A* **33,** 903 (1977).
10. P. VILLARS AND K. GIRGIS, *Acta Crystallogr. Sect. A,* submitted.
11. M. HANSEN, "Constitution of Binary Alloys," McGraw–Hill, New York (1958).
12. R. P. ELLIOTT, "Constitution of Binary Alloys," 1st Suppl., McGraw–Hill, New York (1965).
13. F. A. SHUNK, "Constitution of Binary Alloys," 2nd Suppl., McGraw–Hill, New York (1970).
14. W. B. PEARSON, "A Handbook of Lattice Spacings and Structures of Metals and Alloys," Vol. 1 (1958), Vol. 2 (1967), Pergamon, Oxford.
15. ASTM card index, International Center for Diffraction Data, Philadelphia, Pa. (1979).
16. W. G. MOFFATT, "Handbook of Binary Phase Diagrams," General Electric Company, Schenectady, N.Y. (1978).
17. C. B. SHOEMAKER AND D. P. SHOEMAKER, in "Development in the Structural Chemistry of Alloy Phases" (B. C. Giessen, Ed.), Plenum, New York (1969).
18. A. R. MIEDEMA, *J. Less-Common Met.* **32,** 117 (1973).
19. S. GELLER, *Acta Crystallogr.* **9,** 885 (1956); **10,** 380 (1957).
20. L. PAULING, *Acta Crystallogr.* **10,** 374 (1957).
21. G. R. JOHNSON AND D. H. DOUGLASS, *J. Low-Temp. Phys.* **14,** 565 (1974).
22. D. DEW-HUGHES, *Cryogenics* **15,** 435 (1975).
23. L. R. TESTARDI, *Rev. Mod. Phys.* **47,** 637 (1975).
24. R. M. WATERSTRAT, *J. Less-Common Met.* **43,** 105 (1975).
25. J. MULLER, *Rep. Prog. Phys.* **43,** 641 (1980).
26. F. E. WANG, *J. Solid State Chem.* **6,** 365 (1973).
27. J. T. WABER, K. GSCHNEIDNER, J. A. C. LARSON, AND M. Y. PRINCE, *Trans. AIME* **227,** 718 (1963).